Radiation Physics and Chemistry 106 (2015) 193–198

Contents lists available at ScienceDirect

Radiation Physics and Chemistry

journal homepage: www.elsevier.com/locate/radphyschem

Effect of swift heavy ion irradiation on structural and opto-electrical properties of bi-layer CdS–Bi_2S_3 thin films prepared by solution growth technique at room temperature

Shaheed U. Shaikh [a], Farha Y. Siddiqui [a], Deepali J. Desale [a], Anil V Ghule [a], Fouran Singh [c], Pawan K. Kulriya [c], Ramphal Sharma [a,b,*]

[a] Thin Film and Nanotechnology Laboratory, Department of Physics, Aurangabad, India
[b] Department of Nanotechnology, Dr. Babasaheb Ambedkar Marathwada University, Aurangabad-431004, Maharashtra, India
[c] Inter University Accelerator Center, Aruna Asaf Ali Marg, New Delhi, India

HIGHLIGHTS

- Preparation of samples by chemical bath deposition technique.
- The thin films were annealed in an air atmosphere for 1 h. at 250 °C.
- Annealed sample irradiated by 120 MeV energy Au^{9+} ions at fluence 5×10^{12} ions/cm^2.
- Study of modification induced by air annealing and irradiations.

ARTICLE INFO

Article history:
Received 4 March 2014
Accepted 26 July 2014
Available online 6 August 2014

Keywords:
Thin films
Electrical properties
Optical properties
Chemical synthesis
Ag ion irradiated

ABSTRACT

CdS–Bi_2S_3 bi-layer thin films have been deposited by chemical bath deposition method on Indium Tin Oxide glass substrate at room temperature. The as-deposited thin films were annealed at 250 °C in an air atmosphere for 1 h. An air annealed thin film was irradiated using Au^{9+} ions with the energy of 120 MeV at fluence 5×10^{12} ions/cm^2 using tandem pelletron accelerator. The irradiation induced modifications were studied using X-ray diffraction (XRD), Atomic Force Microscopy (AFM), Raman spectroscopy, UV spectroscopy and *I–V* characteristics. XRD study reveals that the as-deposited thin films were nanocrystalline in nature. The decrease in crystallite size, increase in energy band gap and resistivity were observed after irradiation. Results are explained on the basis of energy deposited by the electronic loss after irradiation. The comparative results of as-deposited, air annealed and irradiated CdS–Bi_2S_3 bi-layer thin films are presented.

1. Introduction

Cadmium sulphide (CdS) and Bismuth sulphide (Bi_2S_3) are n-type semiconductors having the direct energy band gap of 2.48 eV and 1.78 eV, respectively, which belongs to II–VI and V–VI semiconductors. CdS and Bi_2S_3 received great importance due to their potential application in conversion of solar energy into electrical energy. Excellent absorbance, high optical transparency rank them as promising candidates for optical as well as electric applications like solar cell fabrication (Thanachayanont et al., 2008; Sasikala et al., 2000), photosensor (Pouzet et al., 1992) and thermoelectric power (Curran and Phillippe, 1982; Ghosh and Varma, 1979). Few reports are available on preparation and characterization of as-deposited CdS–Bi_2S_3 composite thin film (Dipalee et al., 2012). The modifications or changes induced by post deposition techniques on CdS–Bi_2S_3 bi-layer thin film has not been studied systematically. Thus, in present work we combine the prominent properties of CdS and Bi_2S_3 thin film into a CdS–Bi_2S_3 bi-layer thin film by chemical ion exchange method for synthesizing the stoichiometric composition, homogenous interface and stable nanostructured thin films. Further, effect of annealing and irradiation on prepared bi-layer thin film has been studied.

The SHI is an efficient post deposition treatment, which enables controlled compositional and surface modification in the materials. In this process, an ion impinged on the surface of the thin film looses its energy in the form of elastic and inelastic collisions, which may be used for the excitation of electrons from their atomic levels in the material. Irradiation causes loss in energy by

* Corresponding author at: Thin Film and Nanotechnology Laboratory, Department of Physics, Aurangabad, India. Tel.: +91 9422793173/91 240 2401365; fax: +91 240 2403115/2403335.
E-mail address: rps.phy@gmail.com (R. Sharma).

http://dx.doi.org/10.1016/j.radphyschem.2014.07.017
0969-806X/

two different independent processes, i.e. through nuclear energy loss (S_n) and electronic energy loss (S_e). The effect of electronic stopping power (S_e) dominates over nuclear stopping power (S_n) (Fleischer et al., 1965; Ison et al., 2007). The electronic energy loss is responsible for the inelastic collision in which the atoms of target get excited or ionized. These inelastic collisions result in ionization of the charge carriers and atoms from their molecular levels, which make drastic change in the material by displacing ions from the surface and mixing at an interface. These ionic displacements create vacancies and defects in the material along with creation of ion tracks which may be responsible for surface modifications. The formation of such heavy energy ion tracks indicate the melting, sputtering and resolidification of the material in formation of new bonds and are supposed to be leads to the modifications of materials. This process lead to the formation of point defects, phase transformation, crystallization and amorphization (Ratheesh et al., 2005; Rani et al., 2008). There are only few repots available on irradiation of CdS (Ahire et al., 2007) and Bi_2S_3 (Ahire et al., 2009; Dipalee et al., 2013) thin film.

Therefore in the present work we comparatively studied as-deposited CdS–Bi_2S_3 bi-layer, 250 °C air annealed and irradiated thin films. Irradiation was carried out at 120 MeV Au^{9+} ions at the fluence 5×10^{12} ions/cm^2.

2. Experimental details

2.1. Synthesis

The cadmium solution (0.02 M) was prepared using cadmium sulfate hydrate $CdSO_48H_2$ (pH∼11). Thiourea (CS $(NH_2)_2$ (0.03 M) was used as source of sulfide, the solution of thiourea mixed to cadmium solution with the same pH. The chemically clean ITO glass substrate was dipped in vertical position in prepared alkaline aqueous solution for 3–4 h. CdS thin film has been deposited on Indium Tin Oxide (ITO) glass substrate by Modified chemical Bath Deposition (MCBD) technique at room temperature (Shaikh et al., 2012). Next Bi_2S_3 thin film was grown on previously deposited CdS thin film at room temperature by Successive Ionic Layer Adsorption and Reaction (SILAR) technique (20 cycles). Bismuth nitrate ($Bi(NO_3)_35H_2O$) (0.003 M), (pH∼11) and Thioacetamide (C_2H_5NS) (0.1 M), (pH∼11) were used as source materials for bismuth and sulfide. Thickness of CdS and Bi_2S_3 thin film was measured to be∼350 nm and 200 nm, respectively. The combine thickness of CdS–Bi_2S_3 bi-layer thin film was ∼550 nm. Thickness of thin film was calculated by weight difference method. The prepared bi-layer thin film were annealed at 250 °C for 1 h in air, further the thin film was cut into 1×1 cm^2 area and used as target in the irradiation experiment.

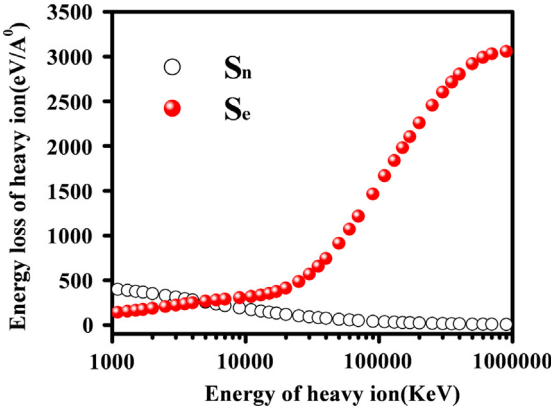

Fig. 1. Energy dependence of electronic and nuclear energy loss of Au9+ ions in CdS–Bi_2S_3 material.

The irradiation experiments were performed on the 15 UD tandem Pelletron at IUAC, New Delhi, India. The thin film was irradiated by 120 MeV Au^{9+} ions with 5×10^{12} ions/cm^2 fluence. The electronic energy loss (S_e) for 120 MeV Au^{9+} ions in CdS–Bi_2S_3 matrix was calculated using the Monte Carlo Code SRIM-2008. The electronic energy loss (S_e) was found 2.189 keV/Å in CdS–Bi_2S_3 bi-layer thin film. Fig. 1 indicates that the electronic energy loss is the dominant mechanism for the gold ions which loses their energy in CdS–Bi_2S_3 bi-layer thin film.

3. Characterization techniques

Pristine, air annealed and irradiated CdS–Bi_2S_3 bi-layer thin films were characterized using different techniques. The thickness of the film was determined by weight gravimetric method, using the density value as 4.82 g/cm^3 for CdS and 6.87 g/cm^3 for Bi_2S_3, respectively. The structural investigation were done by X-ray diffraction (XRD) with glancing angle theta (θ) (θ=5°) with in the range of 20–60° by Bruker AXS X-ray diffractometer, Germany (Model D8Advanced), using Cu-K_α radiation of λ=1.5406 Å in the detector scan mode. Topography of the thin film samples were studied by Atomic force microscopy (AFM) of Digital/Veeco Instrument Inc. Optical study was performed by Perkin Elmer, Lambda 25 spectrophotometer within the range 300 to 1100 nm. Raman spectra in the region 100 to 750 cm^{-1} of the samples were recorded by Raman molecular spectrometer from Renishaw UK. Finally, *I–V* measurements were studied by Lab Equipment model interface with computer by applying silver contacts over the thin film and the results are presented.

4. Result and discussion

4.1. Structural properties

Fig. 2 shows the XRD patterns of pristine, annealed and irradiated samples, respectively. The XRD patterns of samples exhibit an intense peak at 27.71° which can be assigned to the (0 0 2) planes and few less intense peaks at 26.79°, 37.54°, 52.41°, 55.60° and 59.02° associated with (1 0 2), (1 1 2), (0 0 4) and (2 0 2) planes of hexagonal CdS. The peaks of Bi_2S_3 were observed at 25.30°, 28.11°, 45.33° and 49.02° corresponding to the (1 3 1), (1 0 2), (2 0 0), (0 1 6) and (0 0 4) planes of orthorhombic phase. All the remaining high intense peaks attributed to characteristic

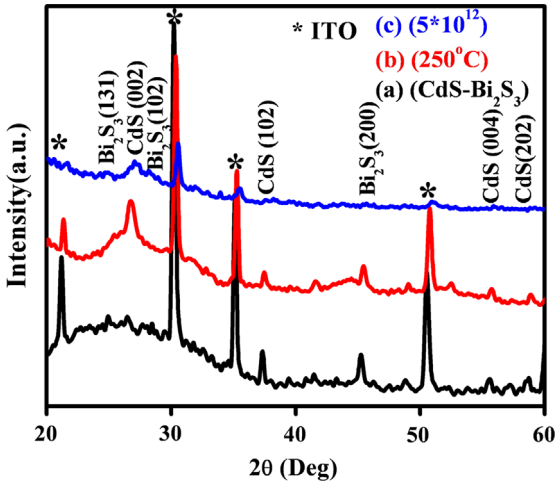

Fig. 2. XRD pattern of (a) pristine (b) annealed and (c) irradiated at 5×10^{12} ions/cm^2 fluence bi-layer thin film of CdS–Bi_2S_3.

peaks of ITO glass substrate. The calculated lattice parameters are in good agreement with the JCPDS data (84-0279 and 80-0006).

The intensity and FWHM of the peaks varied after annealing and irradiation. No additional peaks related to other crystalline phases of CdS and Bi_2S_3 were observed in XRD pattern after annealing and irradiation. This shows the structural stability of CdS and Bi_2S_3 against annealing and irradiation. The amorphization was not observed after irradiation of 120 MeV Au^{9+} ions with fluence 5×10^{12} ions/cm^2. Hence the electronic loss (S_e) might not be sufficient to induce amorphization in CdS–Bi_2S_3 bi-layer thin film, but results in reduction of crystallite size with drastic change in intensity. The average crystallite size has been estimated from the XRD pattern using the Scherrer's formula.

$$D = \frac{k\lambda}{\beta \cos \theta} \quad (1)$$

where, D is the crystallite size, k is shape constant and is equal to 0.94; β is the full width at half maximum (FWHM) and λ is the wavelength of the X-rays. The air annealing of sample results in decrease of FWHM. It is observed that the crystallite size increases with the increase in annealing temperature as a result of agglomeration (Shaikh et al., 2012; Kumar et al., 2010). After irradiation the FWHM was found to be increased, with drastic suppression in all the peaks. The observed decrease in crystallite size and suppression in the peaks at higher fluence this might be due to increase of micro-strains generated by irradiation, which induces the lattice defects. According to coulomb explosion model, phenomenon leads to localized destruction of the lattice. At higher fluence the irradiation produces cylindrical shock waves pushing the atom from their original position and distorting their lattice structure which creates dislocation defects (Agarwal et al., 2006). The dislocation density (δ), defined as length of dislocation lines per unit volume of the crystals, can be estimated from the following relation $\delta = 1\backslash D^2$ where D is the crystallite size (Chandramohan et al., 2009; Williamson and Smallman, 1956). The dislocation density for pristine sample was observed to be reduced after annealing. The decrease in dislocation density might be due to an increase in average crystallite size. Irradiation results increase in δ value, due to decrease in crystallite size through lattice compaction. The formation of lattice compaction is mainly attributed to polygonization. The irradiation induces lattice disorder or dislocation due to polygonization (Tsuchiya et al., 1998; Costantini et al., 2007; Matzke et al., 2000).

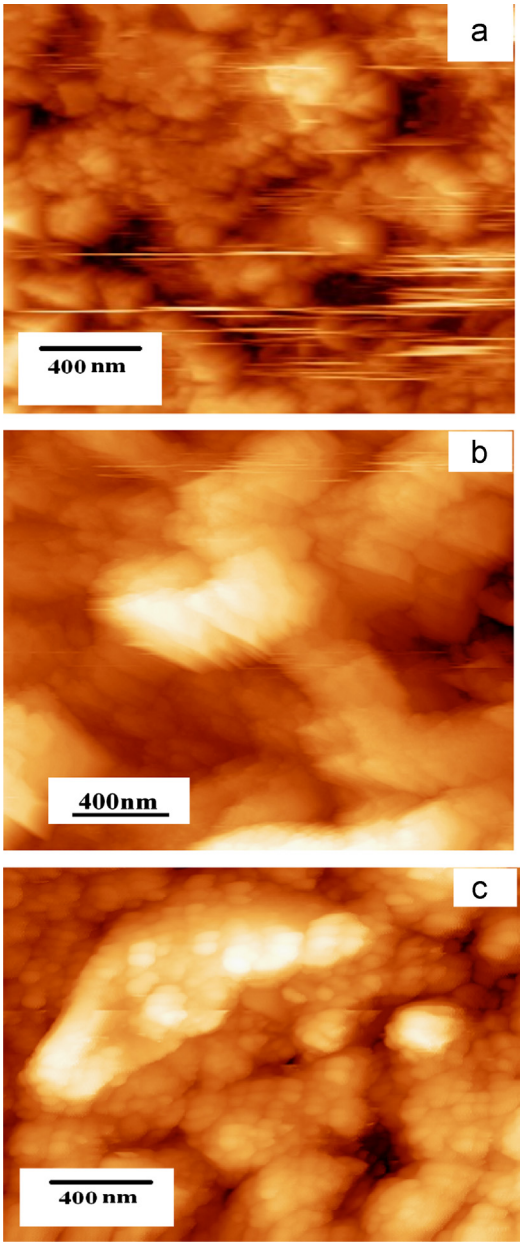

Fig. 3. AFM images of CdS–Bi_2S_3 bi-layer thin film (a) pristine, (b) annealed. and (c) irradiated samples.

4.2. Topographical study

Fig. 3(a)–(c) presents the AFM images for pristine, annealed and irradiated samples, respectively. Fig. 3(a) indicates granular nature of the thin film with the formation of the small grains with large numbers of grain boundaries over the ITO glass substrate. In case of the 250 °C air annealed sample the grain size is found to be enhanced with reduced grain boundaries as compared to pristine sample, which is shown in Fig. 3(b). The annealing process modifies the crystallite structure and size through agglomeration of grains. Annealing involves heating and controlled cooling of material, which enhances the size of the crystal and rearrange them periodically to reduce defects. The process leads to conversion of small grains into larger one or cluster of the grains (Kumar et al., 2010; Nanda et al., 2002; Ahmad et al., 2010).

Fig. 3(c) shows the formation of smaller grains after irradiation in comparison with pristine and annealed sample. The effect of irradiation depends mainly on the range of fluence and material. Irradiation breaks the grain boundaries to form larger or smaller grains, depending on the range of fluence. The decrease in grain size is observed in Fig. 3(c). The observed change in grain size might be due to the subdivisional grain growth through polygonization, which results in an increase of defect density.

The polygonization is the subdivision of large grains into smaller grains due to increase in the stress over the surface. The polygonization is clearly observed after irradiation which can be seen in Fig. 3(c). The smaller grains or sub grains have small missmatch in crystallographic orientation which leads to deformation in the crystal developed after irradiation (Agarwal et al., 2006; Chandramohan et al., 2009). The roughness of the samples is

Table 1
Structural parameters estimated from the XRD pattern of pristine, annealed and SHI irradiated CdS–Bi_2S_3 bi-layer thin films with 120 MeV Au^{9+} ions of 5×10^{12} ions/cm^2 fluencies.

Type	δ (m^{-2})	D (nm)
Pristine	6.94×10^{15}	12
Annealed	2.50×10^{15}	20
Irradiated 5×10^{12} ions/cm^2	1.234×10^{15}	9

found to be changed after annealing and irradiation. The observed roughness was 98, 123.60 and 92.54 nm for pristine, annealed and irradiated samples, respectively. The AFM study showed subdivisional growth in the sample after irradiation at the fluence of 5×10^{12} ions/cm^2 (Table 1).

4.3. Raman spectroscopic studies

The Raman spectra of pristine, annealed and irradiated CdS–Bi_2S_3 bi-layer thin films were taken at room temperature within the range of 100–700 cm^{-1} as shown in Fig. 4. Raman spectra exhibit four distinct vibrational peaks at 121, 300, 446 and 605 cm^{-1} corresponding to the longitudinal optical (LO) phonon modes. The peak positions of CdS spectra are observed at 300 and 600 cm^{-1} corresponding to 1LO (fundamental frequency) and 2LO (first overtone) phonon mode (Zeiri et al., 2007; Rajeev and Abdul, 2008). The peak positions for Bi_2S_3 are observed at 121 cm^{-1} and 446 cm^{-1} corresponding to 1LO and 2LO (Xuelian and Chuanbao, 2008).

The Raman spectrum indicates drastic change in FWHM and intensity after annealing as well as irradiation. There were no shifts observed in peak positions after annealing and irradiation. The enhancement or reduction in the FWHM and intensity of the Raman peaks with annealing and irradiation treatment may be correlated with crystallite size. The intensity of prominent peak observed at 300 cm^{-1} was found to be noticeably increased after annealing and found to decrease after irradiation, which is shown in Fig. 4. The asymmetry and the FWHM increase with the decreasing diameter of nanocrystals (Nandakumara et al., 2001). The decrease in FWHM after short time heating might be due to increase in crystallite size and reduction of defects. Raman study supports the obtained XRD and AFM results.

4.4. Optical studies

Fig. 5 shows the band spectra for pristine, annealed and irradiated samples. Fig. 5(A) shows increase in absorbance after annealing, which specifies the red shift in the material after annealing and modification in top of valence and bottom of conduction band, respectively. We observed reduction in the absorbance of irradiated CdS–Bi_2S_3 bi-layer thin films as compared to the pristine and annealed film. The shift in absorption peak obtained in the spectra might be related to the band to band transitions and the spin orbit splitting (Kale and Lokhande, 2005; Gudage and Sharma, 2010). The spin orbit interaction between

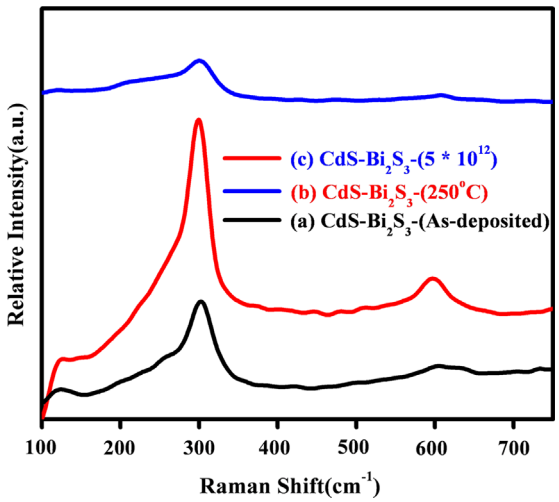

Fig. 4. Raman Spectra of pristine, annealed and irradiated samples.

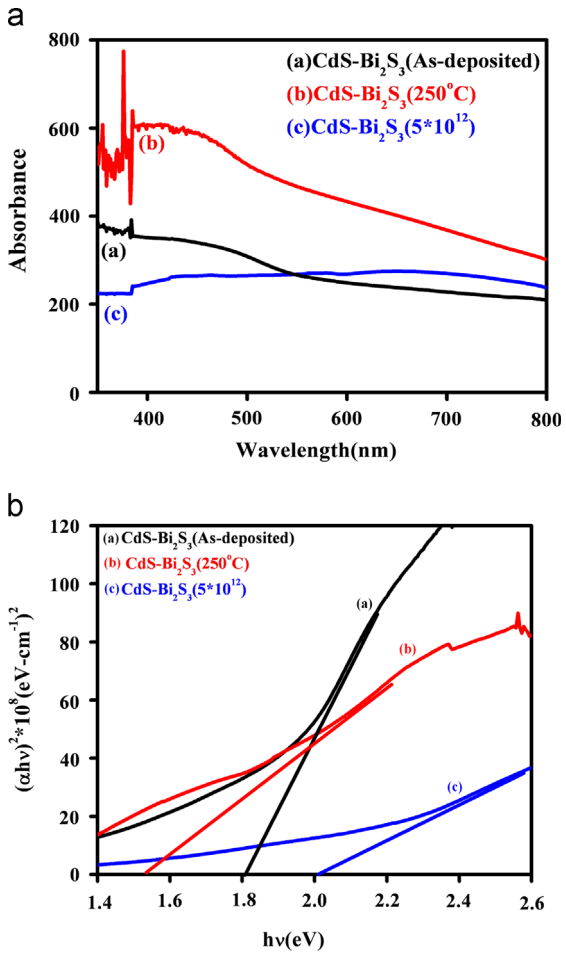

Fig. 5. (A) Optical absorbance and (B) energy band gap for pristine, annealed and irradiated samples.

ions of CdS–Bi_2S_3 bi-layer is expected to be cause for the observed shift in the absorption band edge. The energy band gap of the samples was studied by optical absorption measurement within the range 300–800 nm. The band gap of samples was calculated by plotting graph between $(\alpha h\nu)^2$ against the photon energy $h\nu$, with help of optical absorbance where α is the absorption coefficient, h is the Plank constant and ν is the frequency of incident light. Using Tauc's the absorption coefficient is given by

$$\alpha = \frac{\alpha_0 (h\upsilon - E_g)^n}{h\upsilon} \quad (2)$$

where E_g the energy difference between valence and conduction band and n is a constant equal to 1/2 for direct band gap materials and 2 for indirect band gap material. The natures of the plots indicate the existence of direct transitions. The band gap E_g is determined by extrapolation of the straight portion of the plot to the energy axis as shown in Fig. 5(B). The direct band gap of pristine sample is found to be 1.81 eV and reduces to 1.59 eV after annealing in an air atmosphere at 250 °C for 1 h. The improvement in the crystallites of sample is followed by shift in optical band gap (Ahire et al., 2007). The band gap is found to be increased from 1.59 to 2.02 eV with reduction in absorbance of the material after irradiation. Fig. 5(B) shows enhancement in band gap after irradiation. The change in optical band gap is closely related to crystallite size. The reduction in crystallite size results into enhancement of band gap (Kayanuma, 1988; Sun et al., 2001).

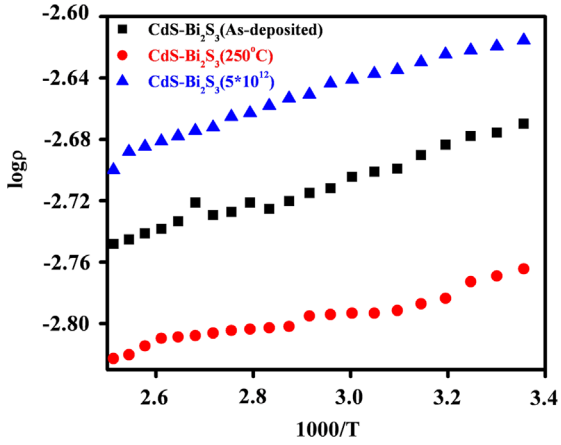

Fig. 6. Schematic representation for pristine, annealed and irradiated samples Arrhenius plot of log$_\rho$

4.5. Electrical studies

Fig. 6shows the variation of logarithm of electrical resistivity (log ρ) with the reciprocal of temperature ($1/T$) for pristine, annealed and irradiated samples, respectively. The calculated room temperature electrical resistivities of pristine, annealed and irradiated samples were 2.9×10^{-3}, 2.1×10^{-3} and $3.3\times10^{-3}\,\Omega$ cm, respectively. The decrease in resistivity after annealing can be correlated with increase in the crystallite size, which reduces the defect density. The annealing effect creates less grain boundaries as compared to irradiation process, which can be observed in AFM images. The formation of larger grain improves the motion of electron through particle to particle after annealing. The activation energy was calculated by using following formula

$$\rho=\rho_0\exp(E_a/KT) \tag{3}$$

where ρ is resistivity at temperature at T, ρ_o is a constant, k is Boltzmann constant. The calculated activation energy for pristine, annealed and irradiated samples were 18×10^{-3}, 12×10^{-3} and 21×10^{-3} V, respectively. The high resistivity and high activation energy in the case of as-deposited and irradiated thin film was observed due to dislocation, lattice imperfection and the creation of deep levels inside the band gap which traps the free carriers (Singh et al., 2001). The grain boundary and trapping center theory was given by Steo and Baccarani. Trapping center at the grain boundaries capture free carriers and these charged centers further create barriers and thus the carrier transport is influenced by created barriers. All these defects cause the decrease in the crystallite size at the growth process. The decrease in the resistivity and activation energy after annealing is due to enhancement in the crystallite size with the reduction of the defects and grain boundaries (Sharma et al., 1992). Annealing process also create the electronic contacts between particles all over thin film (Nanda et al., 2002).

4.6. Photosensitivity

The room temperature I–V characteristic of thin film was studied with the help of current–voltage measurement system. Fig. 7(a)–(c) shows I–V characteristics of pristine annealed and irradiated samples in dark and illumination condition (60 W), respectively. The photo-current was found to increase after annealing and decrease after irradiation. I–V curves are straight lines passing through the origin indicating ohmic behavior. Changes in I–V graphs with respect to intensity of light indicates photosensing phenomenon, hence these samples may be useful for photosensor applications. The photosensitivity (Ahire et al., 2007) of sample in the presence of light intensity were calculated

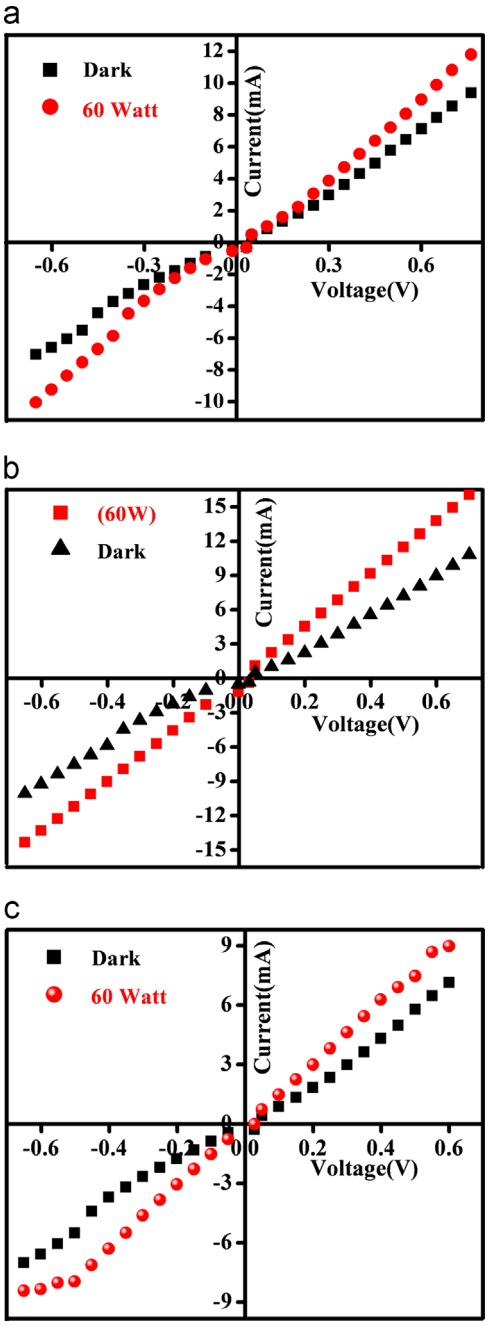

Fig. 7. IV graph for (a) pristine, (b) annealed and (c) irradiated samples.

by the formula

$$S=\frac{R_d-R_l}{R_d} \tag{4}$$

where R_d is resistance of thin film in dark, R_l is resistance of thin film in the presence of light.

The calculated values of photosensitivity in natural and 60 W light are 0.32, 0.43 and 0.28 for pristine, annealed and irradiated samples, respectively. Comparable values have been obtain in study of CdS quantum dots (Shaikh et al., 2012) and Bi_2S_3 thin film (Dipalee et al., 2013).

The increase in absorbance and enhancement in crystallite size after annealing were found to be effective to enhance the absorptive power and surface area of the sample. This provides immense space for light trapping as compared to pristine sample. The decrease in the resistivity due reduction in defects also supports

enhancement in photosensitivity. The illuminated light results in increased photocurrent of the sample (Orton et al., 1982). Photocurrent decreased after irradiation. This may also be correlated with roughness as estimated from AFM study, which provides less surface area for photon trapping as compared to annealed sample. The observed results are consistent with the report (Tripathi and Srivastava, 2007). The annealed sample showed good photo response as compared to irradiated sample.

5. Conclusions

CdS–Bi_2S_3 bi-layer thin films have been successfully deposited by chemical method. XRD and AFM study of annealed sample showed enhancement in grain size with reduction in band gap and resistivity whereas irradiated sample displays decrease in grain size leading to enhancement in band gap and resistivity of the thin film. The structural modifications observed from the XRD pattern, which are correlated with the Raman spectra. The absorbance after annealing increased and decreased after irradiation. From the observed results we may conclude that the air annealing enhances the properties whereas Au^{9+} ions irradiation at the fluence 5×10^{12} ions/cm^2 with 120 MeV energy produces defects in CdS–Bi_2S_3 bi-layer thin films.

Acknowledgements

Authors acknowledge, UGC, New Delhi for providing fellowship and financial support in the form of research project Ref. No: F No 33–398/2007(SR) and UGC-DAE Scientific consortium Indore for providing characterizations. We are thankful to the Director, IUAC, New Delhi and Dept. of Physics Dr. Babasaheb Ambedkar Marathwada University, Aurangabad for providing lab facilities.

References

Agarwal, DC, Amit, K, Khan, SA, Kabiraj, D, Singh, F, Tripathi, A, Pivin, JC, Chauhan, RS, Avasthi, DK., 2006. SHI induced modification of ZnO thin film Optical and structural studies. Nucl. Instrum. Methods Phys. Res., Sect. B 244, 136–140.

Ahire, RR, Sagade, AA, Deshpande, NG, Chavhan, SD, Sharma, R, Singh, F., 2007. Engineering of nanocrystalline cadmium sulfide thin films by using swift heavy ions. J. Phys. D: Appl. Phys 40, 4850–4854.

Ahire, RR, Sagade, AA, Chavhan, SD, Huse, V, Gudage, YG, Singh, F, Avasthi, DK, Phase, DM, Sharma, R., 2009. Modifications of structural, optical and electrical properties of nanocrystalline bismuth sulphide by using swift heavy ions. Curr. Appl. Phys. 9, 374–379.

Ahmad, MK, Halid, MLM, Rasheid, NA, Ahmed, AZ, Abdullah, S, Rusop, M., 2010. Effect of annealing temperatures on surface morphology and electrical properties of titanium dioxide thin films prepared by sol gel method. J. Sustainable Energy Environ 1, 17–20.

Chandramohan, S, Sathyamoorthy, R, Sudhagar, P, Kanjilal, D, Kabiraj, D, Asokan, K, Ganesan, V, Shripathi, T, Deshpande, UP., 2009. High-energy heavy-ion induced physical and surface-chemical modifications in polycrystalline cadmium sulfide thin films. Appl. Phys. A 94, 703–714.

Costantini, JM, Trautmann, C, Thome, L, Jagielski, J, Beuneu, F., 2007. Swift heavy ion-induced swelling and damage in yttria-stabilized zirconia. J. Appl. Phys. 101, 073501–073509.

Curran JS, Phillippe R. In: Proceedings of the 14th International Conference on ECPV Solar Energy, Stresa, 1982. 10–14.

Dipalee, JD, Shaheed, S, Arindam, G, Ravikiran, B, Farha, S, Anil, G, Ramphal, BS., 2012. Preparation and characterization of CdS–Bi_2S_3 nanocomposite thin film by successive ionic layer adsorption and reaction (SILAR) method. Composites Part B 43, 1095–1100.

Dipalee, JD, Shaheed, S, Arindam, G, Ravikiran, B, Farha, S, Anil, G, Ramphal, BS., 2013. Enhancement of photosensitivity by annealing in Bi_2S_3 thin films grown using SILAR method. Composites Part B 46, 1–6.

Fleischer, RL, Price, PB, Walker, RM., 1965. Ion explosion spike mechanism for formation of charged particle tracks in solids. J. Appl. Phys. 36, 3645–3652.

Ghosh, G, Varma, BP., 1979. Optical and electrical properties of doped and undoped Bi_2S_3)-PVA films prepared by chemical drop method. Solid State Commun. 31, 683–687.

Gudage, YG, Sharma, R., 2010. Growth kinetics and photoelectrochemical (PEC) performance of cadmium selenide thin films: pH and substrate effect. Curr. Appl. Phys. 10, 1062–1070.

Ison, VV, Ranga Rao, A, Dutta, V, Avasthi, DK., 2007. Effect of swift heavy ion irradiation on spray deposited CdX (X=S,Te) thin films. Nucl. Instr. Meth. B 262, 204–209.

Kale, RB, Lokhande, CD., 2005. Band gap shift, structural characterization and phase transformation of CdSe thin films from nanocrystalline cubic to hexagonal nanorods on air annealing. Semicond. Sci. Technol. 20, 1–9.

Kayanuma, Y., 1988. Quantum-size effects… with spherical shape. Phys. Rev. B: Condens. Matter 38, 9797–9805.

Kumar, P, Jain, N, Agrawal, RK., 2010. Effect of substrate temperature on optical properties of Bi_2S_3 chalcogenide thin films. Chalcogenide Lett. 7, 89–94.

Matzke, H, Lucuta, PG, Wiss, T., 2000. Swift heavy ion and fission damage effects in UO_2. Nucl. Instrum. Methods Phys. Res., Sect. B 166-167, 920–926.

Nanda, KK, Kruis, FE, Fissan, H., 2002. Evaporation of free PbS nanoparticles: evidence of the Kelvin effect. Phys. Rev. Lett. 89 (256103-256101-256103-256104).

Nandakumara, P, Vijayan, C, Rajalakshmi, M, Arora, AK, Murti, YVGS., 2001. Raman spectra of CdS nanocrystals in Nafion: longitudinal optical and con$ned acoustic phonon modes. Physica E 11, 377–383.

Orton, JW, Goldsmith, BJ, Chapman, JA, Powell, MJ., 1982. The mechanism of photoconductivity in polycrystalline cadmium sulphide layers. J. Appl. Phys. 53, 1602–1614.

Pouzet, J, Bernede, JC, Khellil, A, Essaidi, H, Benhida, S., 1992. Preparation and characterization of tungsten diselenide thin films. Thin Solid Films 208, 252–259.

Rajeev, RP, Abdul, MK., 2008. Study of optical phonon modes of CdS nanoparticles using Raman spectroscopy. Bull. Mater. Sci. 31, 511–515.

Rani, S, Puri, NK, Roy, SC, Bhatnagar, MC, Kanjilal, D., 2008. Effect of swift heavy ion irradiation on structure, optical, and gas sensing properties of SnO_2 thin films. Nucl. Instr. Meth. B 266, 1987–1992.

Ratheesh, PM, Kumar, C, Sudha, K, Vijayakumar, KP., 2005. Modifications of ZnO thin films under dense electronic excitation. J. Appl. Phys. 97, 013509–013515.

Sasikala, G, Thilakan, P, Subramanian, C., 2000. Modification in the chemical bath deposition apparatus, growth and characterization of CdS semiconducting thin films for photovoltaic applications. Sol. Energy Mater. Sol. Cells 62, 275–293.

Shaikh, SU, Desale, DJ, Siddiqui, FY, Arindam, G, Birajadar, RB, Ghule, AV, Sharma, R., 2012. Effects of air annealing on CdS quantum dots thin film grown at room temperature by CBD technique intended for photosensor applications. Mater. Res. Bull. 47, 3440–3444.

Sharma, KC, Sharma, RP, Garg, JC., 1992. Structural electrical and optical properties of solution grown polycrystalline $Cu_{1-x}Ag_xSe$ thin films. J. Phys. D: Appl. Phys. 25, 1019–1025.

Singh, R, Arora, SK, Singh, JP, Tyagi, R, Agarwal, SK, Kanjilal, D., 2001. Experimental investigation of 200 MeV 107Ag14+ ion induced modifications in n-GaAs epitaxial layer by in situ resistivity and Hall measurements. Mater. Sci. Eng., B 86, 228–231.

Sun, CQ, Sun, XW, Tay, BK, Lau, SP, Huang, H, Li, S., 2001. Dielectric suppression and its effect on photoabsorption of nanometric semiconductors. J. Phys. D: Appl. Phys. 34, 2359–2362.

Thanachayanont, C, Inpor, K, Sahasithiwat, S, Meeyoo, V., 2008. MEH-PPV/CdS nanorod polymer solar cells. J. Korean Phys. Soc. 52, 1540–1544.

Tripathi, JK, Srivastava, PC., 2007. Effect of swift (100 MeV) heavy ion irradiation on surface morphology and electronic transport in Fe film on Si substrate. Appl. Surf. Sci. 253, 8689–8694.

Tsuchiya, B, Yamamoto, S, Narumi, K, Aoki, Y, Naramoto, H, Morita, K., 1998. Ion irradiation effect on single-crystalline Cu/Nb and Nb/Cu/Nb layers on sapphire. Thin Solid Films 335, 134–137.

Williamson, GK, Smallman, RE., 1956. Philos. Mag. 1, 34–45.

Xuelian, Y, Chuanbao, C., 2008. Photoresponse and field-emission properties of bismuth sulfide nanoflowers. Cryst. Growth Des. 8, 3951–3955.

Zeiri, L, Patla, I, Acharya, S, Golan, Y, Efrima, S., 2007. Raman spectroscopy of ultranarrow CdS nanostructures. J. Phys. Chem. C 111, 11843–11848.